Chapter 5

Synthesis and characterizations of pristine and doped SnO_2 and TiO_2 nanoparticles

---

5.1 Titanium dioxide (TiO_2) nanoparticles

5.1.1. Synthesis

The Titanium dioxide nanoparticles (TiO2) were synthesized using wet chemical method. We have used Titanium Tetrachloride ($TiCl_4$) as Titanium precursor. In addition, ethylene glycol, sodium acetate and polyethylene glycol were used to prepare nano TiO_2. All the chemicals were of analytical grade and used without further purification. In first step, 40ml of ethylene glycol was kept in round bottom flask and drop-wise $TiCl_4$ has been added to this solution under continuous stirring at room temperature. This process was continued till solution becomes transparent. After that, sodium acetate (3.6g) and polyethylene glycol (1ml) have been added to this mixture at room temperature and stirred for another 30min. Temperature of reaction increases until condensation in mixture starts. It is indicated by change in the color of mixture from transparent to creamy yellow. Then stirring was continued for another 3 hours. After that, precipitates have been collected by centrifugation and washed 3-4 times with hot distilled water. The last wash was performed with methanol in order to remove water molecules. Finally precipitates were dried in oven at 100^0C overnight. XRD result of this as prepared TiO_2 (TN0) confirms its amorphous nature. Then it was annealed at 300 ^{0}C and 400 ^{0}C respectively for 2 hours and named as TN1 and TN2 samples [5.1].

5.1.2. XRD Results

X-ray diffraction (XRD) analysis was used to identify and confirm the structure of TiO_2. The average crystallite size can also be determined from XRD pattern of the sample. Fig. 5.1 shows XRD analysis result of TN0 sample. No diffraction peaks were found in XRD pattern suggesting amorphous nature of the sample.

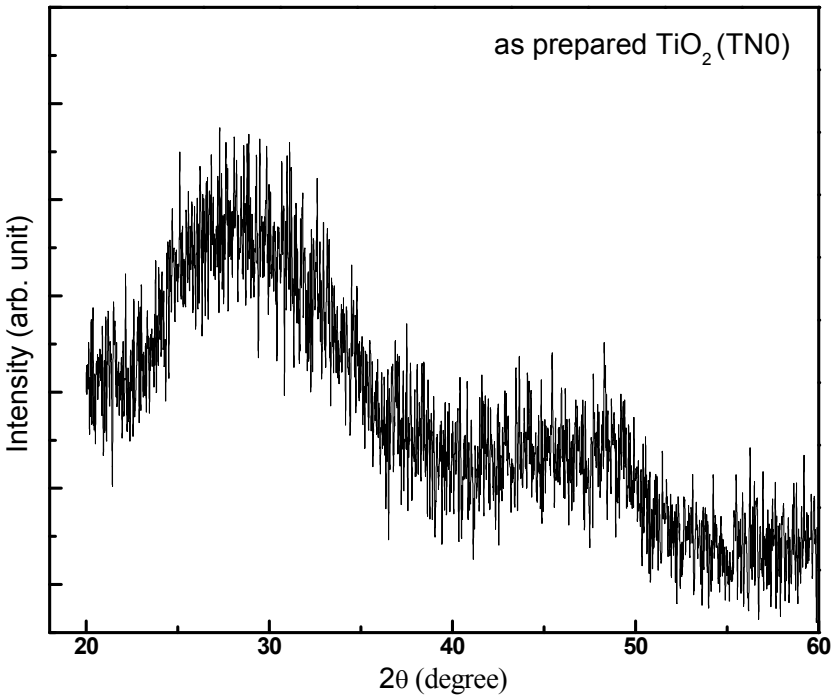

Fig. 5.1 XRD pattern of TiO_2 after drying in oven

The XRD patterns of annealed sample at 300 ^{0}C and 400 ^{0}C are shown below in figs. 5.2 and 5.3.

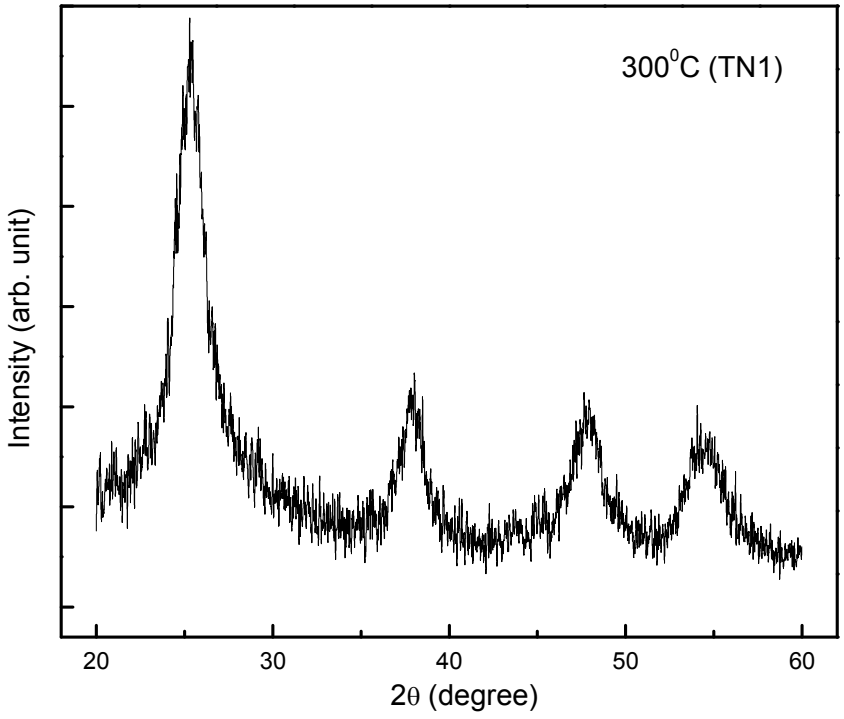

Fig. 5.2 XRD pattern of TiO_2 annealed at 300^{0}C

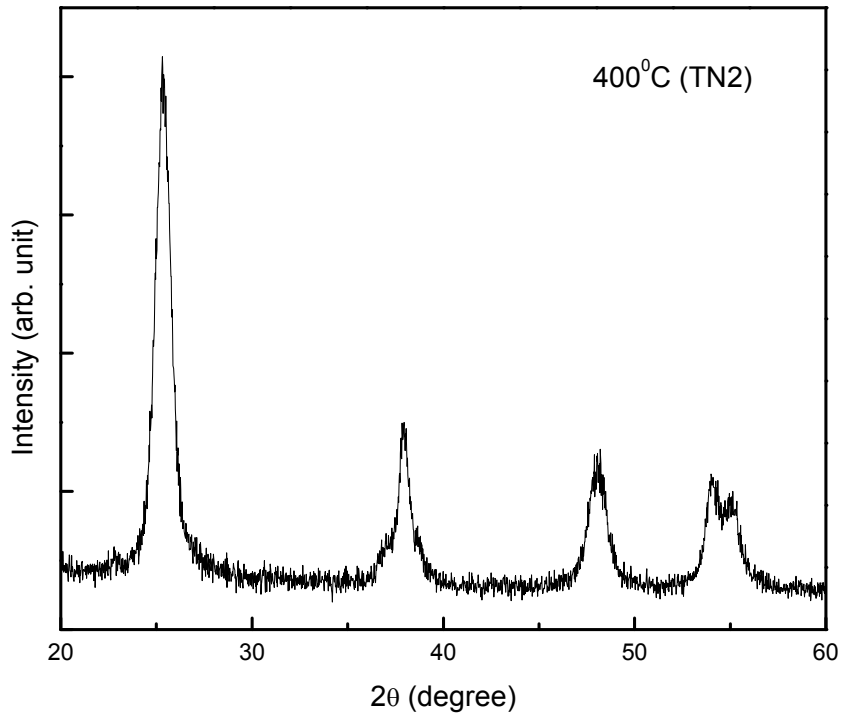

Fig. 5.3 XRD pattern of TiO_2 annealed at 400^{0}C

In fig. 5.3, diffraction peaks at 2θ values of 25.31, 37.94 and 48.11 suggest formation of anatase phase in TiO_2 [5.2]. There were no extra peaks found indicating any impurity in sample. Average crystallite size in both prepared samples were calculated using Scherrer equation [5.3],

$$d = K\lambda / \beta\cos\theta \quad \ldots (1)$$

where, d is average size of grains

K is instrument constant=0.9

λ is Cu wavelength=1.5418 A^0

β=Full width at half maxima of most intense peak

θ=Diffraction angle

From eqn.(1), particle size in TN1 is 4.4 nm and TN2 is 9.0 nm.

5.2 Tin dioxide (SnO_2) nanoparticles

5.2.1. Synthesis

Tin dioxide (SnO_2) nanopowders were synthesized by sol-gel method. We have used Stannous chloride dihydrate ($SnCl_2 \cdot 2H_2O$) (Merck) as tin precursor. In a typical synthesis, 2.0

gms of $SnCl_2 \cdot 2H_2O$ is dissolved in distilled water. Then diluted ammonia (25% NH_4OH) was added drop-wise to the above stirring solution within 30-35 min to get pH of 8.5-8.7. After 30 min again pH was checked and maintained same as before. Here the dropping rate of ammonia must be well controlled for chemical homogeneity. Stirring was continued for another half an hour at room temperature. The resulting opal gel was collected by filtration, successively wash with de ionized water to remove any unreacted salt and excess ammonia. Finally it was dried at 80°C for several hours in air oven. . Heating treatments of the synthesized SnO_2 nanopowders were conducted at 200°C, 400°C, and 600°C for 2 hours, respectively [5.4].

5.2.2. XRD Results

Fig. 5.4(a-c) shows the XRD patterns of SnO_2 nanopowders obtained at different temperature.

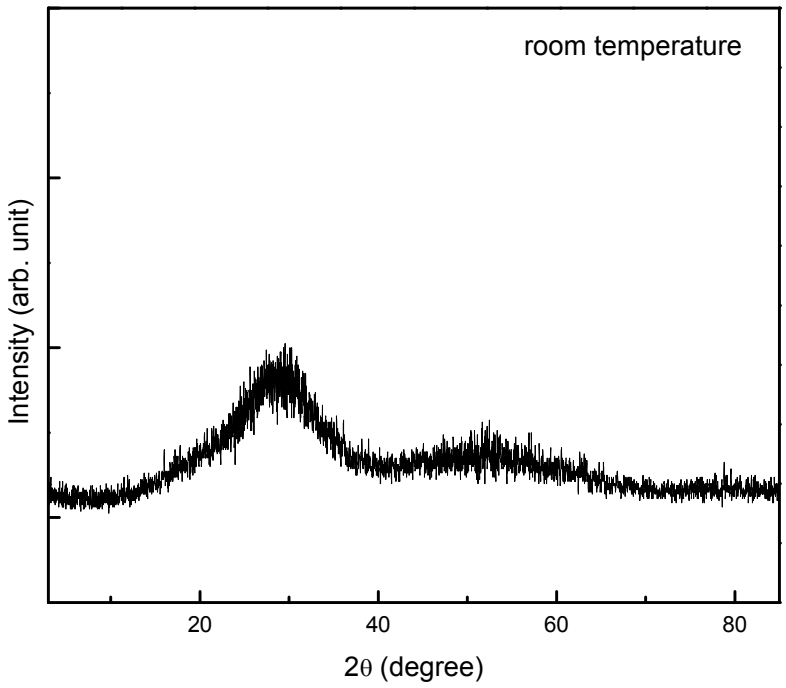

Fig. 5.4 (a) SnO_2 at room temperature

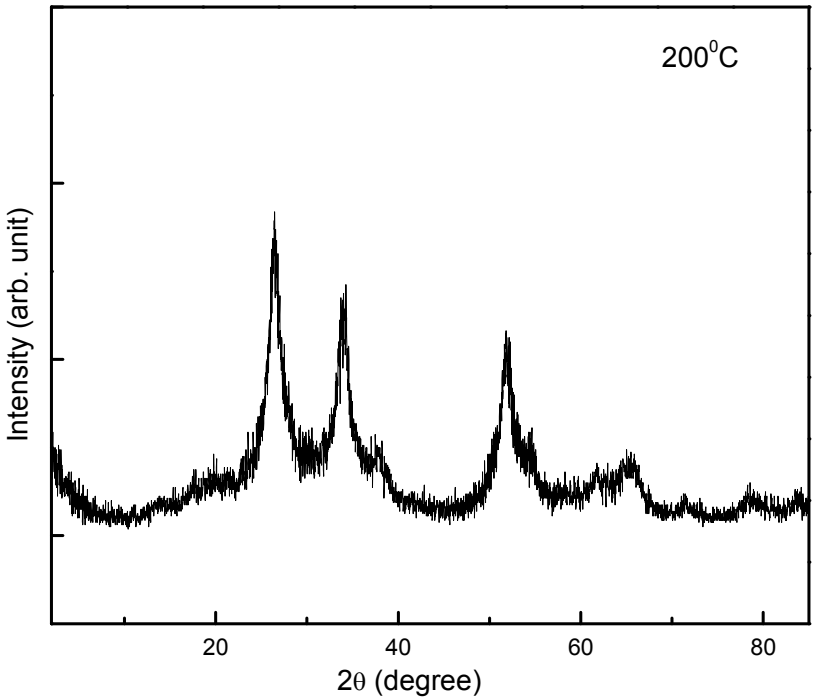

Fig. 5.4 (b) annealed at 200^{0}C temperature

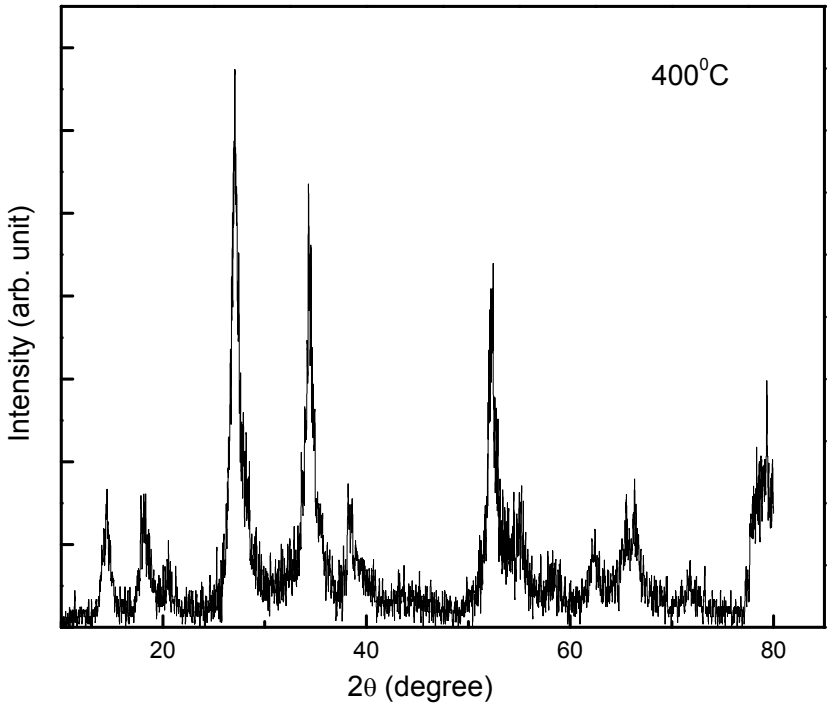

Fig. 5.4 (c) annealed at 400^{0}C temperature

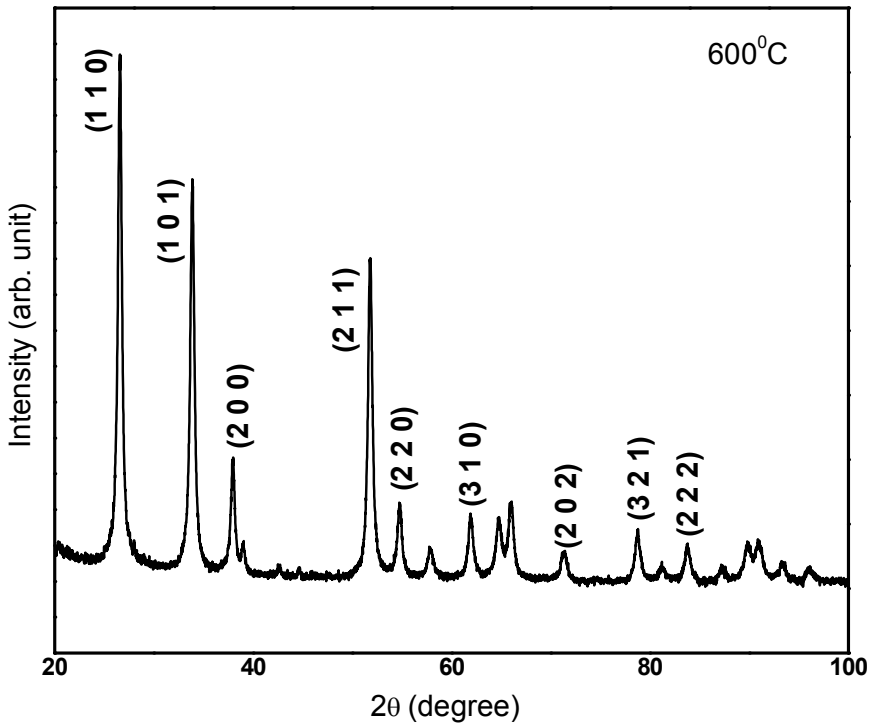

Fig. 5.4 (d) annealed at 600^{0}C temperature

Fig.5.4 nano SnO_2 annealed at different temperatures

Fig. 5.4(a) depicts XRD pattern before heat treatment, SnO_2 nano powder shows amorphous nature. Crystallization starts when temperature of this as-prepared sample increases. At 200^{0}C and 400^{0}C diffraction peaks were observed correspond to SnO_2 crystal structure. As shown in fig. 5.4 (d) at 600^{0}C intense diffraction peaks and different planes are observed. All the peaks match well with standard JCPDS card no. 21-1250 which indicates SnO_2 cassiterite structure as shown in below table 5.1 [5.5].

[Table 5.1]

Comparison of SnO_2 XRD data with JCPDS card.21-1250

JCPDS card 21-1250		**Prepared sample**			**Plane identification**
d	**I/I_0**	**d**	**I/I_0**	**2θ**	
3.35	100	3.35	100	26.55	(1 1 0)
2.64	80	2.64	77.73	33.84	(1 0 1)
2.37	20	2.37	22.42	37.92	(2 0 0)
1.77	70	1.76	66.45	57.25	(2 1 1)
1.68	20	1.67	15	54.71	(2 2 0)

JCPDS card 21-1250		Prepared sample			Plane identification
d	I/I_0	d	I/I_0	2θ	
1.50	10	1.59	6.09	57.82	(0 0 2)
1.42	20	1.49	13.06	61.87	(3 1 0)
		1.43	11.63	64.70	(1 1 2)
		1.41	15.65	65.93	(3 0 1)

Crystallite size was calculated using Scherrer formula and it is observed that as temperature increases size of SnO_2 increases and width of the peaks decreases because of the crystal growth [5.6]. Fig. 5.5 presents comparison of SnO_2 nanoparticles annealed at different temperatures.

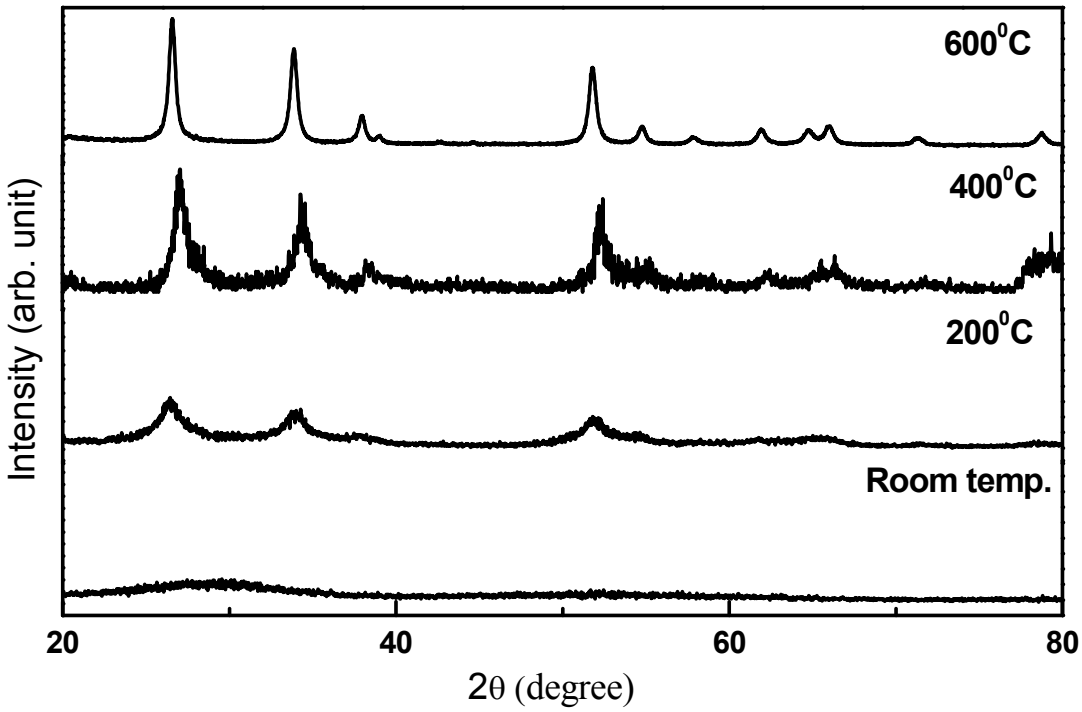

Fig.5.5 Comparison of SnO_2 nanoparticles annealed at different temperatures.

In ideal case, perfect crystal should be extended in all directions to infinity. But practically all crystals have finite size. This fact results in broadening of diffraction peaks. From peak analysis it is found that two major effects are responsible for the broadening in XRD peaks: a) small crystallite size and b) lattice strain. Crystal imperfection and mechanical alloying

cause large amount of strain in nanocrystals [5.7-5.9]. Williamson-Hall plot is a simple analytical method to study size-induced and strain-induced broadening in diffraction peaks using width of the peak as a function of 2θ [5.10].In this section, W-H plot for each sample is drawn to estimate strain in prepared nanocrystals.

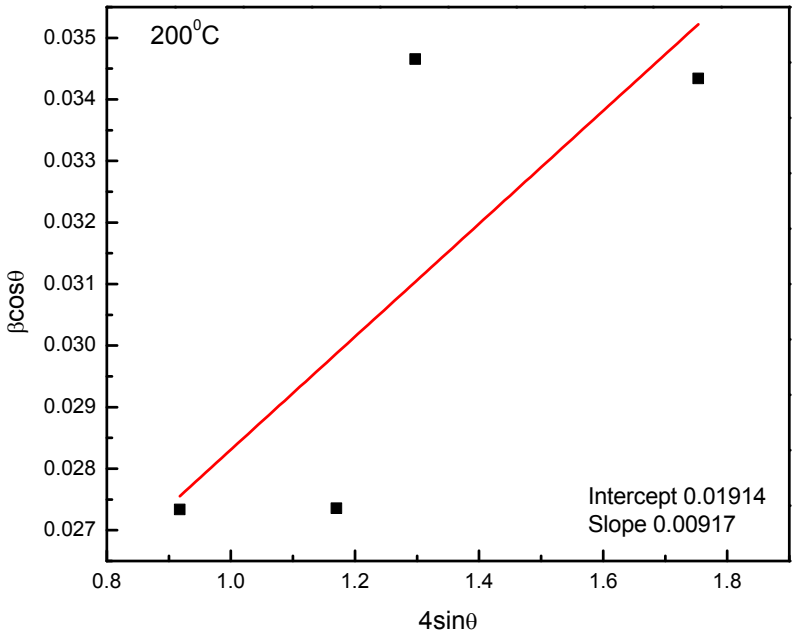

Fig. 5.6 (a) W-H plot for SnO_2 annealed at 200^0C

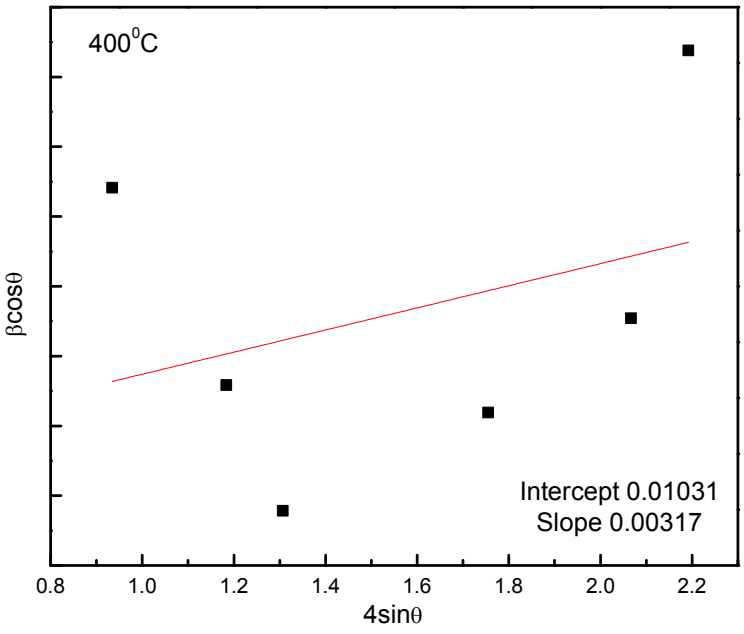

Fig. 5.6 (b) W-H plot for SnO_2 annealed at 400^0C

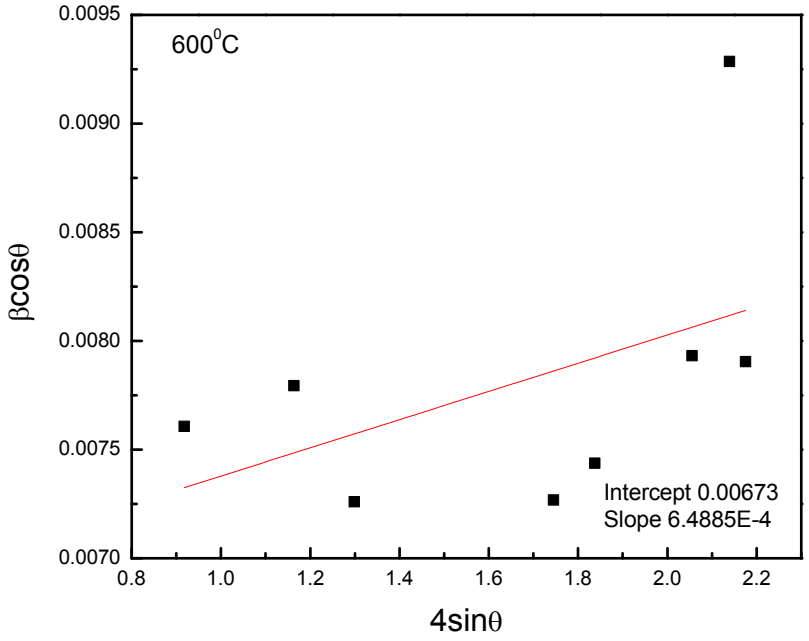

Fig. 5.6 (c) W-H plot for SnO_2 annealed at 600^{0}C

Following table shows comparison of crystallite size in SnO_2 calculated by Scherrer equation and W-H plot respectively. Results obtained from W-H plot are in agreement with that of the crystallite size calculated from Scherrer equation.

[Table 5.2]

Details of crystallite size in SnO_2 nanocrystals using two different methods

Annealing temp. of SnO_2	Average crystallite size (scherrer eqn.) (nm)	Average crystallite size (Williamson-hall method) (nm)
200 ^{0}C	5.07	7.24
400 ^{0}C	6.18	7.36
600 ^{0}C	18.22	20.60

5.2.3 Differential Scanning Calorimetry (DSC) study

The thermal analysis was carried out using Shimadzu-50 DSC instrument in the temperature range from 35^{0}C to 560^{0}C in an oxygen atmosphere with a heating rate of 10^0

C/min. The DSC thermo gram of as prepared SnO_2 nanoparticles (at room temperature) is presented in figure 5.7.

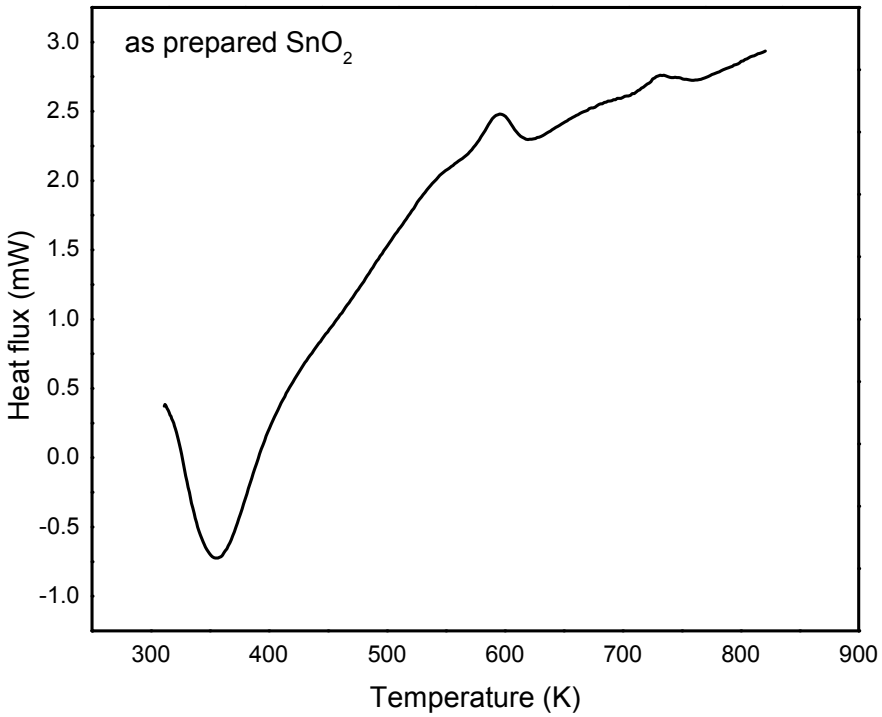

Fig. 5.7 DSC curve of SnO_2 prepared at room temperature

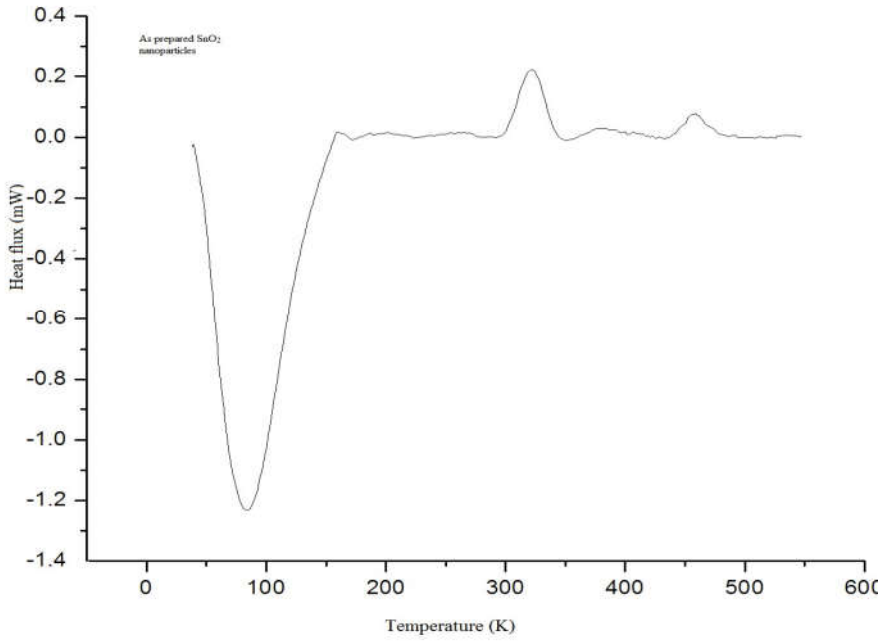

Fig. 5.8 Baseline corrected DSC curve of SnO_2 prepared at room temperature

The DSC curves in figs. 5.7 and 5.8 reveal endothermic peak at 355K and exothermic peak at 595K. The endothermic peak is due to dehydration of precursor and exothermic peak suggests decomposition of chloride ions. Phase formation of SnO_2 nanocrystal is indicated by exothermic peak at 730 K [5.11].

5.2.4 Scanning Electron Microscopy (SEM)

Fig. 5.9 shows SEM image of prepared SnO_2 nanoparticles. JEOL JSM-5610LV scanning electron microscope used at operating voltage of 15 KV to scan the image. It shows that nanoparticles are highly agglomerated. They have irregular shape and are non uniformly distributed.

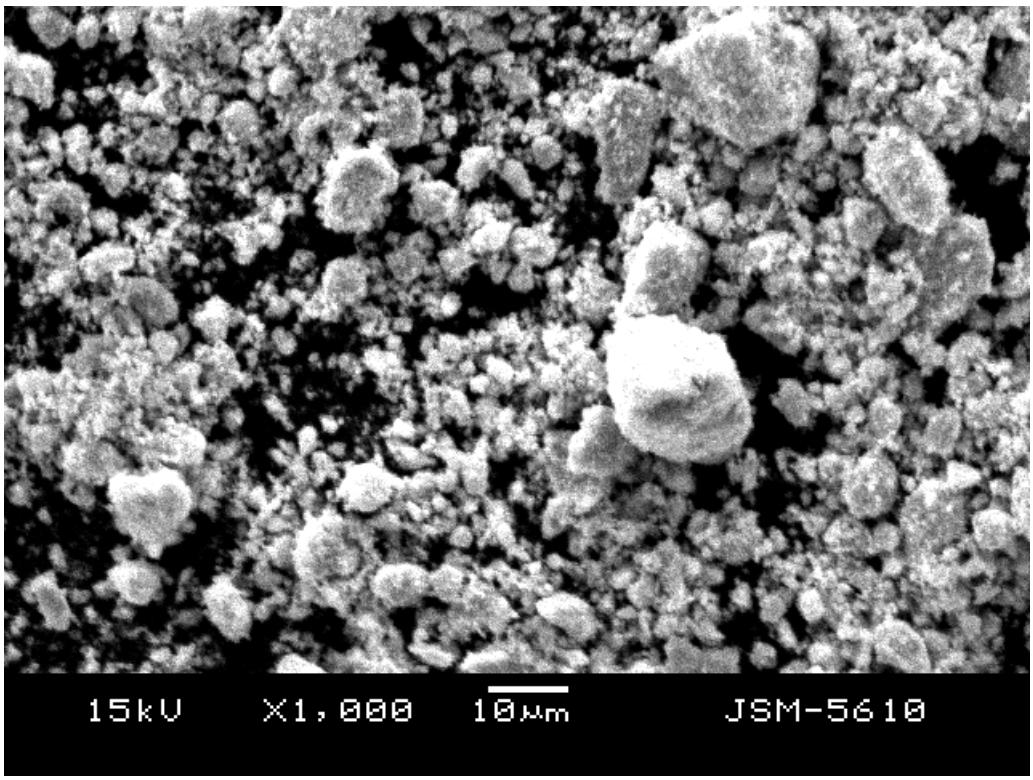

Fig. 5.9 SEM image of SnO_2 nanoparticles

5.3 Iron (Fe) doped Tin dioxide (SnO_2) nanoparticles

The doping of iron in nano sized SnO_2 can enhance electrical and optical properties [5.12]. Fe is a transition metal and when doped in non magnetic semiconductor (SnO_2) it

behaves as a dilute magnetic semiconductor (DMS). This· class of material offer wide range of applications in the field of storage, communication, quantum computation and multi-functionality on a single chip [5.13, 5.14].

5.3.1 Synthesis

Fe doped SnO_2 has been synthesized using precipitation method. Stannous chloride di-hydrate ($SnCl_2 \cdot 2H_2O$) and iron (III) chloride ($FeCl_3$) are used as tin and iron precursors. First 0.005M of $FeCl_3$ solution was added drop-wise into the $SnCl_2 \cdot 2H_2O$ solution and then sodium hydroxide (NaOH) solution was added at room temperature under vigorous stirring which leads to formation of precipitates. Later the precipitates were collected and washed 3-4 times with distilled water using centrifuge. Precipitates were dried in oven at 80^0C overnight and then annealed at 200^0C for 2 hours [5.4].

5.3.2 Characterizations

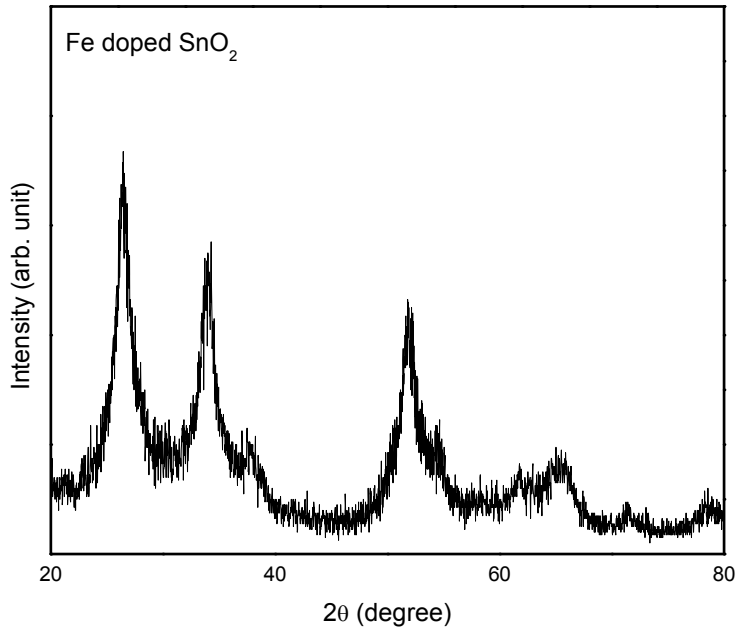

Fig. 5.10 XRD pattern of Fe doped SnO_2 nanoparticles

Fig. 5.10 presents XRD analysis of prepared sample. Diffraction peaks match well with cassiterite structure of SnO_2. It shows Fe is incorporated into SnO_2 crystals and no

impurity peaks are observed such as Sn metal and iron oxide. Crystallite size calculated from Scherrer formula is 7.35 nm. The EDS analysis was performed to analyze chemical composition of the structure. It confirms presence of Fe in SnO_2 nano powder. Atomic % of Fe is 2.83 and weight % is 5.60 as shown in table [5.3]. Morphology of the sample has been studied using SEM analysis. It shows irregular shape of particles with high agglomeration.

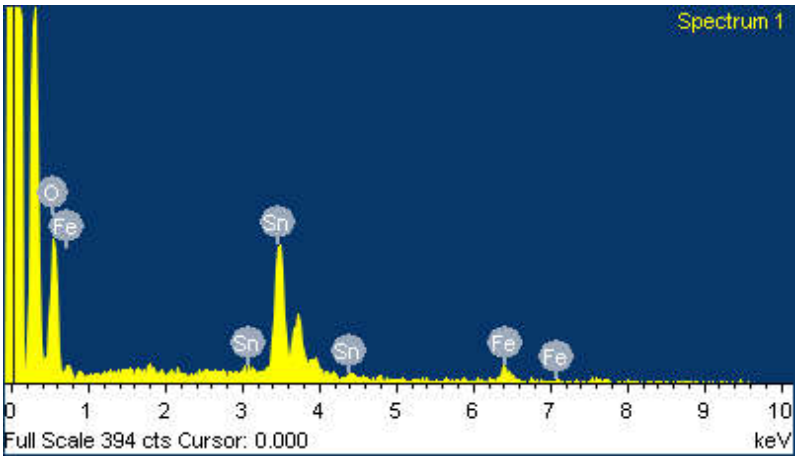

Fig. 5.11 EDS spectra of Fe doped SnO_2

[Table 5.3]

Chemical composition of Fe doped SnO_2

Element	Weight (%)	Atomic (%)
O K	48.84	86.31
Fe K	5.60	2.83
Sn L	45.56	10.85

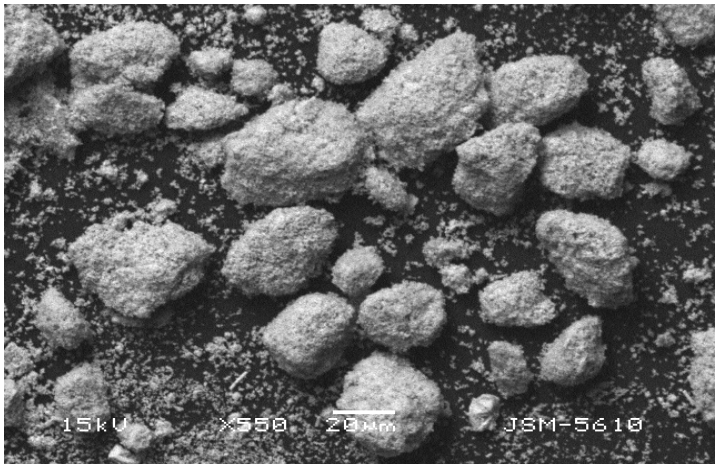

Fig.5.12 SEM image of Fe doped SnO_2

5.4 Ag-SnO_2 nanocomposites

Silver-metal oxides is a very important class of material that can be used as a electrical contact material in general electronic devices such as contactors, relays, circuit breakers and switches [5.15-5.19]. Since past few years Ag-SnO_2 based contact materials have emerged as environment-friendly materials and they have replaced hazardous Ag-CdO. But their commercial production and applications are still limited as their performance in not satisfactory in high temperature region [5.15]. It can be solved by increasing dispersion in Ag-SnO_2 particles when synthesized using proper condition and route. Mechanical alloying is one of the effective methods to achieve homogeneous distribution of particles and thereby high dispersion in metal-oxide matrix [5.20, 5.21]. In present work, Ag-SnO_2 nanocomposites were prepared using powder metallurgy (ball milling) method.

5.4.1 Process

We used pure SnO_2 nano powder prepared by wet chemical method and commercial micron sized Ag metal powder as starting materials. Weight ratio of starting powders Ag: SnO2 is taken to 92:8 [5.22]. The Ag-92 wt. % SnO_2 nano-composite powder was synthesized by high energy milling in a planetary ball mill. Milling was achieved in 250ml capacity twin-bowl type planetary ball mill of M/s Insmart systems. In milling process, tungsten carbide lined stainless steel vials and tungsten carbide balls of 10mm and 16 mm are used as grinding media. The mill was operated at a speed of 400 rpm and ball to powder ratio was fixed to 10:1. The powder sample was collected after every 1 hour during the course of milling for the purpose of XRD analysis. After 3 hours of milling Ag-SnO_2 powder was kept in vacuum oven at 150^0C for 1 hour.

To form bulk solid sample (pellets), after milling Ag-SnO_2 nanocomposites powder was pressed on a 100 ton capacity hydraulic press at 2 ton pressure in single action die compaction mode. We have calculated theoretical density of pellets and to examine effect of sintering it was again calculated after sintering. Sintering is a kind of heat treatment to compact powder and enhance strength and integrity. Because of this, constituent atoms diffuse across the boundary of particles and sufficient strength is achieved [5.23]. The prepared nanocomposites are subjected to sintering at temperature 850^0C for 1.5 hours under vacuum furnace of 10^{-2} torr. The heating rate was fixed of 7^0C per minute. Temperature was

monitored on microprocessor based temperature controller model WEST-2050 of M/s Toshniwal Brothers Pvt. Ltd. The sintered pellets were repressed at a pressure of 7 ton [5.24].

5.4.2 Characterizations

5.4.2.1 XRD analysis

The XRD results of powder samples after 1, 2 and 3 hours of milling are given below. All three samples contain diffraction peaks corresponding to pure silver and SnO_2. No extra peaks were found indicating any impurity or other phase formation in Ag-SnO_2 composites.

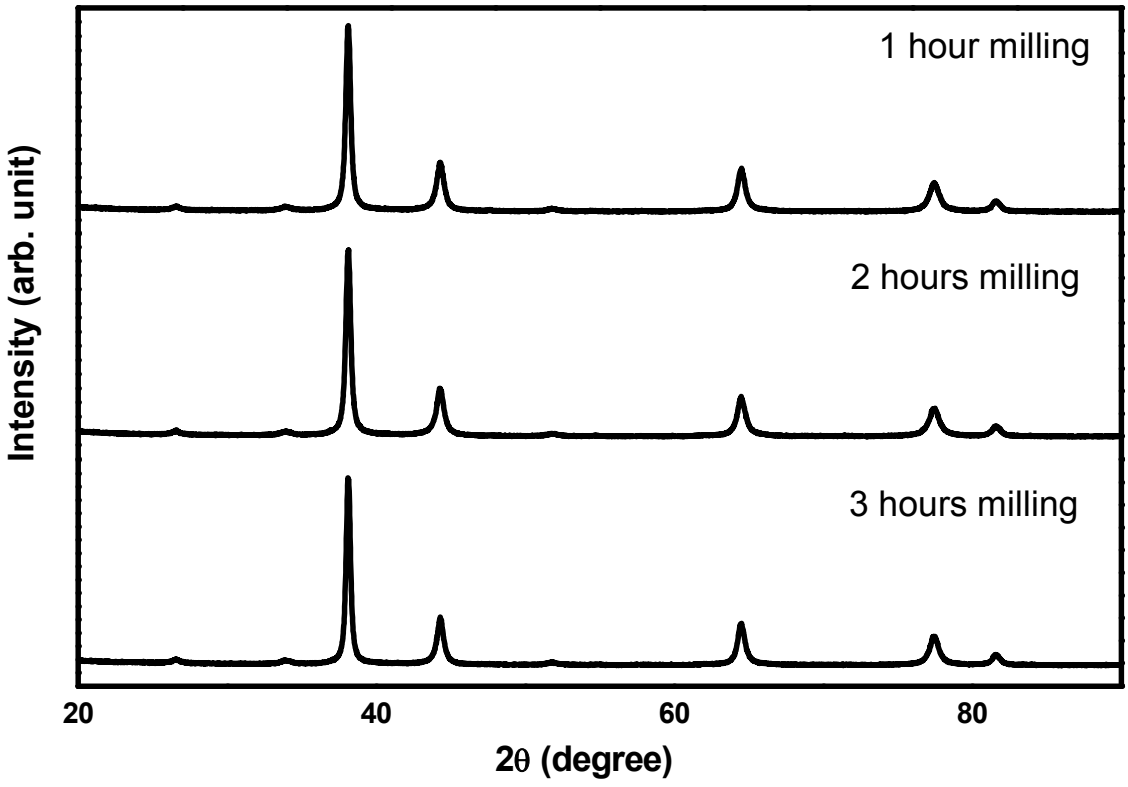

Fig. 5.13 XRD patterns of Ag-SnO_2 nanocomposites after milling of different time

Hall-Williamson plots are obtained from XRD data. Crystallite size in Ag-SnO_2 nanocomposites are calculated from both Scherrer formula and Williamson-Hall (W-H) plot. Size obtained from W-H plot shows higher value than calculated from Scherrer eqn. which is

obvious because of the strain effect in sample. Comparison of these data is given in below table, below.

[Table 5.4]

Calculated crystallite size of Ag-SnO_2 nano composites

Ag-SnO_2 nano composites	Crystallite size from Scherrer eqn. (nm)	Crystallite size from Williamson- hall plot (nm)
1 hour milled	29.56	66.65
2 hours milled	38.65	110
3 hours milled	39.37	61.05

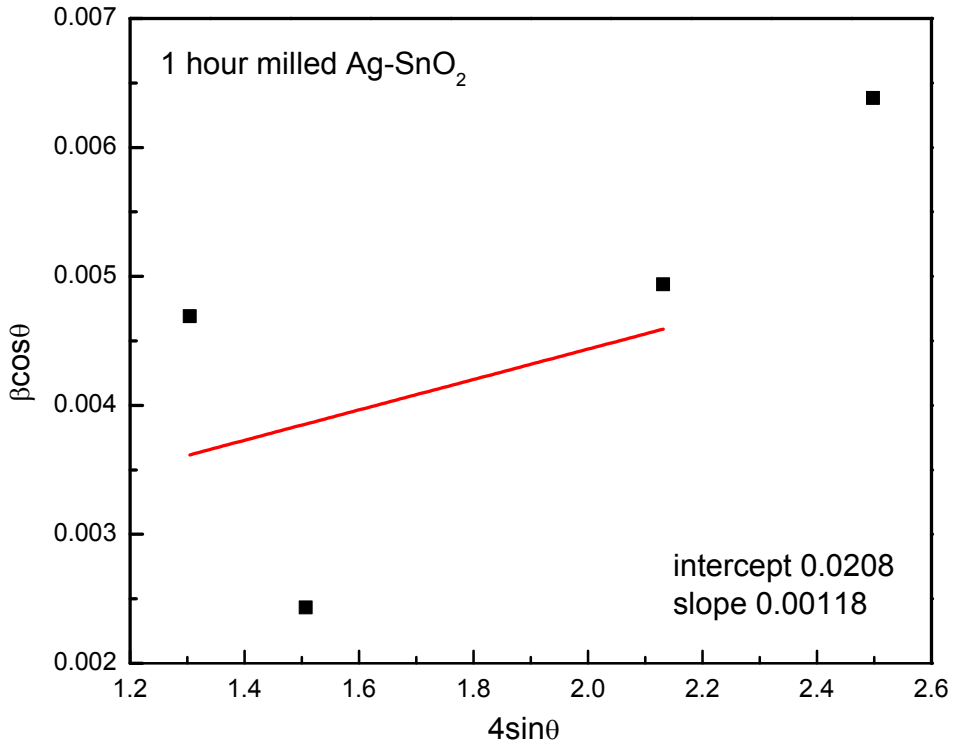

Fig. 5.14 (a) 1 hour milling

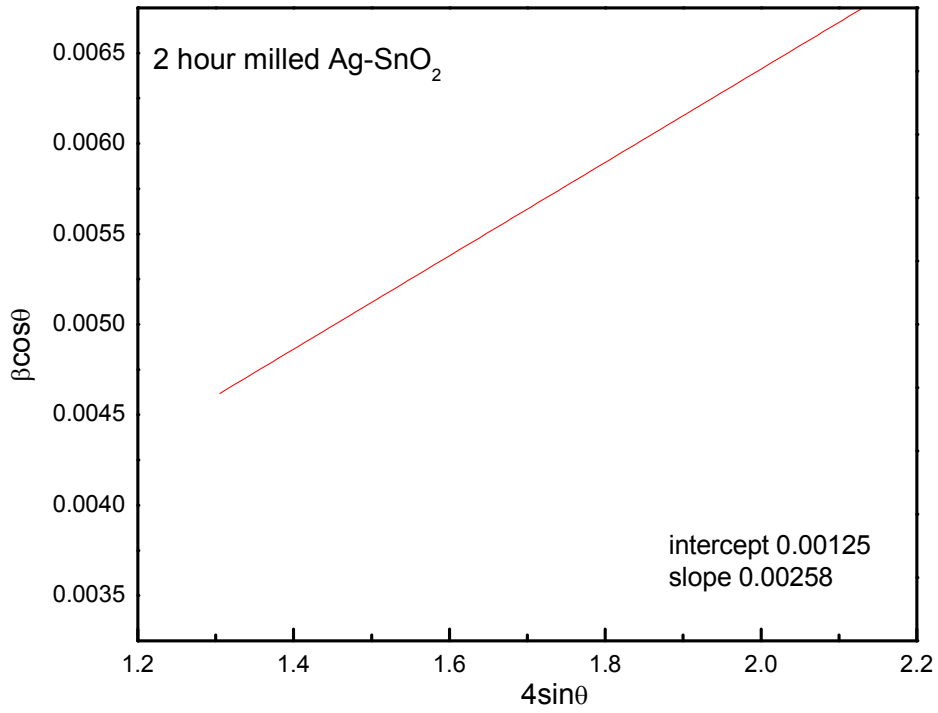

Fig. 5.14 (b) 2hours milling

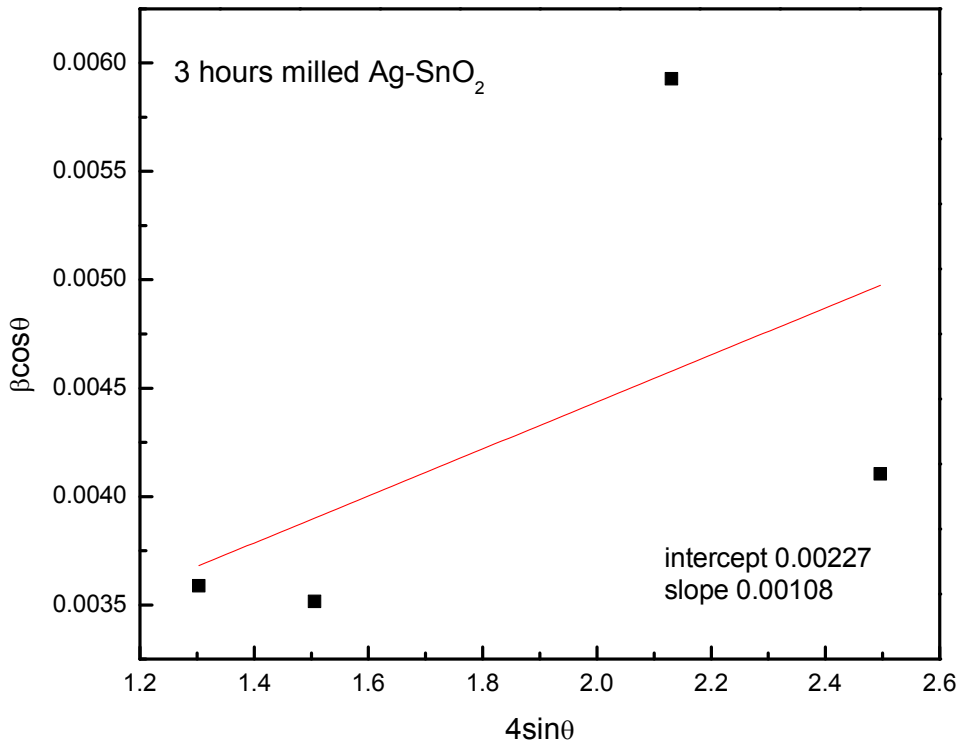

Fig. 5.14 (c) 3hours milling

5.4.2.2 Density results

Density is derived from dimensions and mass of pellets. After sintering and repressing value of density increases which is obvious because of the integrity and close binding of constituent atoms. In other words, we can say that one can achieve density very close to its theoretical value by sintering in proper conditions.

[Table 5.5]

(a) Density of Ag-SnO_2 nanocomposites before sintering

Sample (pellet) no.	Thickness (cm)	Diameter (cm)	Volume (cm^3)	Mass (gm)	Density (gm/cm^3)(%)	Theoretical density (%)
1	0.237	1.006	0.1883	1.4874	7.899	78.37
2	0.238	1.006	0.1890	1.4851	7.857	77.96
3	0.238	1.006	0.1890	1.4876	7.8708	78.09

(b) Density of Ag-SnO_2 nanocomposites after sintering

Sample (pellet) no.	Thickness (cm)	Diameter (cm)	Volume (cm^3)	Mass (gm)	Density (gm/cm^3)	Theoretical density (%)
1	0.233	0.9406	0.1618	1.4409	8.9054	88.35
2	0.241	0.9403	0.1672	1.4364	8.5897	85.22
3	0.240	0.9383	0.1657	1.4365	8.6692	86.01

(c) Density of Ag-SnO_2 nanocomposites after re-pressing

Sample (pellet) no.	Thickness (cm)	Diameter (cm)	Volume (cm^3)	Mass (gm)	Density (gm/cm^3)	Theoretical density (%)
1	0.194	0.1009	0.1549	1.4119	9.1426	90.70
2	0.192	0.1006	0.1525	1.4162	9.2865	92.13

5.4.2.3 Micro-hardness measurement

Vicker microhardness of prepared pellet was measured at Electrical Research and Development Association (ERDA), Vadodara. For the measurement applied test force was 0.490 N (50 gf). We have obtained micro hardness measurement on surface of Ag-SnO_2 pellet to be 124 HV 0.05.

References

5.1 R. Desai, S.K. Gupta, S. Mishra, P.K. Jha and A. Pratap, Int. J. of Nanosci. **10,** 1249 (2011).

5.2 T.A.AL-Dhahir, Diyala J. for pure sci. **9,** 108 (2013).

5.3 https://en.wikipedia.org/wiki/Scherrer_equation.

5.4 S. Sohila, M. Rajalakshmi, C. Muthamizhchelvan, and S. Kalavathi, AIP. Conf. Proc. **1447,** 251 (2012).

5.5 Powder Diffraction File (Inorganic Compounds), Hanwalt Method Search Manual (1977).

5.6 A. Gaber, M. A. Abdel- Rahim, A. Y. Abdel-Latief, Mahmoud. N. Abdel-Salam, Int. J. Electrochem. Sci. **9,** 81 (2014).

5.7 V.D. Mote, Y. Purushotham and B.N. Dole, . J of Theor. and Appl. Phy. **6:6,** 1 (2012).

5.8 T. Ungar, J. Mater. Sci. **42,** 1584 (2007).

5.9 C. Suryanarayana, Mechanical Alloying and Milling. Marcel Dekker, New York (2004).

5.10 C. Suryanarayana, Grant Norton, M: X-ray Diffraction: A Practical Approach. Springer, New York (1998).

5.11 S. Xiaolan, L. Dongfeng, Z. Yimeng, D. Yi, L. Mei, W. Shunkui, H. Xi, Q. Yixin, J of Wuhan Uni. of Tech.-Mater. Sci. **25,** 929 (2010).

5.12 . J. X. Deng, Y. F. Tian, S.S. Yan, Q. Cao, G.L. Liu, Y. X. Chen, L.M. Mei, G. Ji & Z. Zhang, J. Appl. Phys. **104,** 013905 (2008).

5.13 A. Sharma, M. Varshney, S. Kumar, K.D.Verma and R. Kumar, Nanomater. nanotechnol., **1,** 24 (2011).

5.14 David D. Awschalom and Michael E. Flatté, Nat. Phys. **3,** 153 (2007).

5.15 V. Ćosović, N. Talijan, D. Živković, D. Minić, Ž. Živković, J. Min. Metall. Sect. B-Metall.**48,** 131 (2012).

5.16 M. Sato, M. Hijikata, Trans JIM, **23,** 267 (1982).

5.17 P.C. Wingert, C.H. Leung, IEEE Trans CHMT, **12,** 16 (1989).

5.18 A. Pandey, P. Verma, O.P. Pandey, Ind. J. Eng. Mater. Sci., **15,** 236 (2008).

5.19 M. Braunović, N.K. Myshkin, V.V. Konchits, Electrical contacts: Fundamentals, Applications and Technology, CRC Press, Taylor and Francis Group, 2007.

5.20 V. Ćosović, M. Pavlović, A. Ćosović, P. Vulić, M. Premović, D. Živković5, N. Talijan, Sci. of Sint, **45,** 173 (2013).

5.21 F. Heringhaus, P. Braumann, D. Ruhlicke, E. Susnik, R. Wolmer, , Proc. 20th Int. Conf. on Electr. Contact Phenom., Stockholm, 199 (2000).

5.22 V. Cosovic´, A.C´. osovic´, N. Talijan, D. Z˘ivkovic´, D. Manasijevic ´, D. Minic, J of Alloys and Comp. **567,** 33 (2013).

5.23 http://www.ipmd.net/Introduction_to_powder_metallurgy/Sintering

5.24 B.R. Rehani, P.B. Joshi and V.K. Kaushik, Ind. J. of Engg. and Mater. Sci. **16,** 281 (2009).